A01-16414

AIAA 2001–0542

SENSOR INTEGRATION FOR INFLIGHT ICING CHARACTERIZATION USING NEURAL NETWORKS

James W. Melody, Devesh Pokhariyal, Jason Merret,
Tamer Başar, William R. Perkins, Michael B. Bragg,
University of Illinois,
Urbana, IL

39th AIAA Aerospace Sciences Meeting and Exhibit
January 8–11, 2001
Reno, Nevada

AIAA 2001-0542

SENSOR INTEGRATION FOR INFLIGHT ICING CHARACTERIZATION USING NEURAL NETWORKS

James W. Melody*, Devesh Pokhariyal†, Jason Merret†,
Tamer Başar‡, William R. Perkins‡, Michael B. Bragg§,
University of Illinois,
Urbana, IL

This work advances a neural network that characterizes aircraft ice accretion in order to improve flight performance and safety. Neural networks have been developed previously for use within an ice management system that monitors inflight aircraft icing and its effects upon performance, stability, and control. The previous work has applied these networks to stability and control derivative estimates provided by an H^∞ parameter identification algorithm during a longitudinal maneuver. This paper extends those results by addressing ice characterization in the *absence of pilot input* when poor excitation of the flight dynamics limits the accuracy of parameter estimates. To compensate for this shortcoming inherent to steady-level flight scenarios, the neural network presented in this paper integrates steady-state characterization and hinge moment sensing with parameter estimates. The neural network provides icing characterization in terms of an estimate of the previously developed icing severity factor, η. Extensive simulation results are presented that indicate the accuracy of neural network characterization during steady-level flight in the presence of sensor noise and turbulence over a broad range of flight trim conditions and turbulence levels. Furthermore, the relative utility of each information source is investigated via consideration of network accuracy of networks trained only on that information source.

INTRODUCTION

Current aviation research and development has begun to focus more upon creating aircraft that are safe and reliable during severe weather conditions. Aircraft icing is a large area of concern due to the detrimental effects of accumulated ice upon aerodynamic performance. Small amounts of ice can have an extreme impact upon aircraft dynamics and consequently, icing has been one of the most visible causes of severe accidents. Icing was determined to be a factor in 803 aircraft accidents that occurred between 1975 and 1988.[1] Nearly half of these accidents resulted in fatalities. Commercial accidents such as the American Eagle ATR-72 crash near Roselawn, Indiana, which killed 68 people in October 1994, have also led to national recognition of icing problems.[2] In response to the abundance of aircraft icing accidents, NASA and the President's Commission on Aviation Safety and Security have developed an aviation safety research plan that places a high national priority upon icing protection and prevention.[3]

Most icing-related accidents occur because ice accretion affects the performance and stability of an aircraft by altering the shape of its aerodynamic surfaces. Other icing incidents include engine failure and propeller ice, but this work will focus only on the effects of airframe icing. Currently, there are two main approaches that deal with the dangers of ice accretion. First, pilots are given complete weather information before and during flights in order to avoid potential icing conditions. Second, aircraft are thoroughly deiced before take-off and then operate an ice protection system (IPS) to accomplish in-flight ice removal.

An IPS functions in either an advisory or primary capacity. Advisory systems rely upon the flight crew to activate ice protection devices based upon data received from icing and environmental sensors. On most commuter aircraft, icing sensors are not available and pilots determine the level of ice accretion by visual inspection of the wings and control surfaces. This type of visual ice detection is inadequate because pilots usually cannot see all of the wing or any of the tail. Systems that function in a primary capacity utilize information from icing sensors to automatically activate

*Graduate Research Assistant, Department of Electrical and Computer Engineering and the Coordinated Science Laboratory, Member AIAA.

†Graduate Research Assistant, Department of Aeronautical and Astronautical Engineering, Member AIAA.

‡Professor, Department of Electrical and Computer Engineering and the Coordinated Science Laboratory.

§Professor and Head, Department of Aeronautical and Astronautical Engineering, Associate Fellow, AIAA.

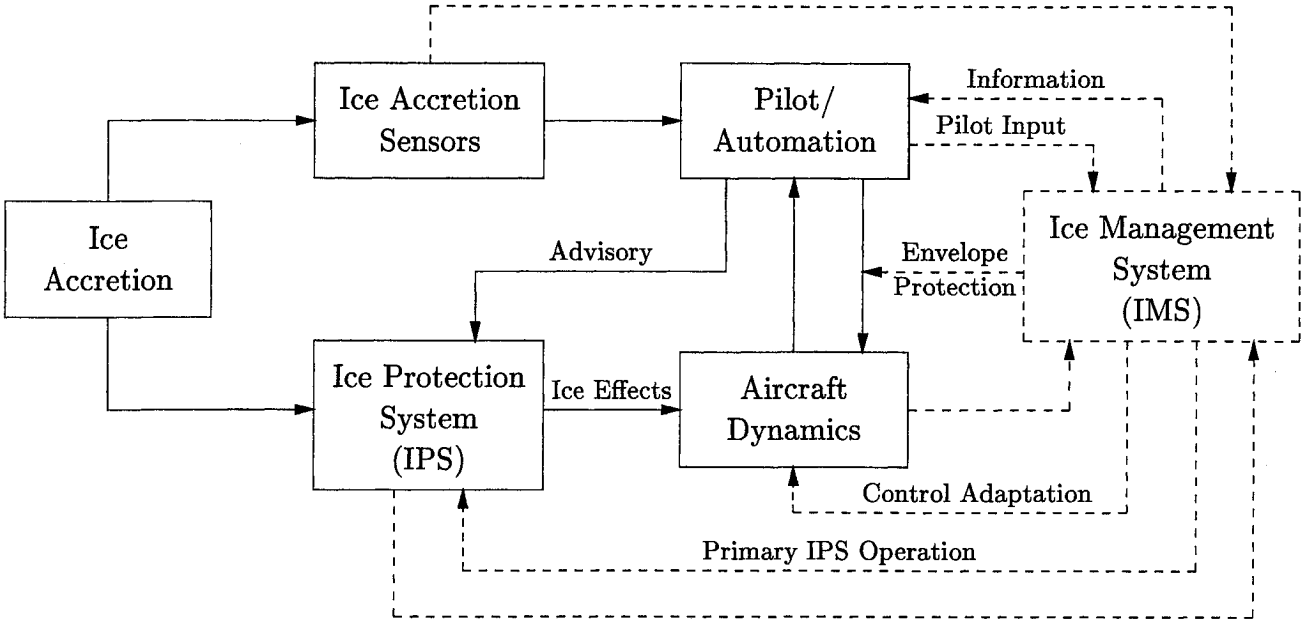

Fig. 1 Aircraft icing encounter model.

anti-ice and de-icing devices. The flight crew is given updates concerning IPS status and may manually override the system. Current ice protection equipment consists mainly of devices that bleed hot engine exhaust onto the wings to prevent icing or inflatable boots that break off accumulated ice.

Recent icing accidents have shown that the IPS approach does not always adequately provide safe and reliable flight during icing conditions. In fact, the ATR-72 accident resulted from ice that accreted aft of the wing de-icing system.[4] In response to the deficiencies of the current IPS, a new approach has been introduced.[2] This approach adds a new Ice Management System (IMS) that works in cooperation with the existing IPS. The purpose of the IMS is to continually monitor ice accretion and its effects, automatically operate the existing IPS and provide the flight crew with an assessment of the aerodynamic performance. It may also adapt flight controls to allow safe and reliable flight through icing conditions.

Ice Management System

The IMS approach is being developed by the University of Illinois Icing Center and is a cooperative effort among researchers from several disciplines including control systems, aerodynamics, flight dynamics, and human factors.[2] The objective of the IMS is to provide an additional layer of defense that guards against aircraft icing accidents. This objective is accomplished by monitoring ice accretion and its effects upon aircraft flight dynamics. The IMS works in cooperation with existing ice protection systems and the flight crew in order to effectively use all available data. A block diagram depicting the operation of the IMS during an icing encounter is shown in Figure 1. The solid lines portray the current state of the art and the dashed lines show the additional capability provided by the IMS. The IMS adds complexity but also creates an aircraft that is much more robust to the effects of ice accretion.

The purpose of the IMS is to allow safe and controllable flight when hazardous icing conditions cannot be avoided. The IMS accomplishes this task by performing three main functions. First, ice must be detected and then classified in order to determine the detrimental effects upon aircraft stability and control. Second, the IPS must be automatically activated and operated while the IMS provides the pilot with continual updates concerning aircraft performance. Third, the flight envelope and aircraft control laws may be adjusted when severe ice creates potentially uncontrollable conditions. This allows the IMS to protect the aircraft against traditional icing handling events such as roll upset and tailplane stall. Following envelope modification, the flight crew will be notified and can then successfully navigate using limited maneuvers until the icing conditions are eliminated.

Effective IMS performance depends heavily upon accurate detection and classification of icing events. Since icing is a concern precisely to the extent that it affects the flight dynamics, parameter identification of the flight dynamics is a critical element of the IMS.[5,6] Exhaustive simulation results have demonstrated the superior robustness and convergence properties of H^∞ identification techniques in the presence of disturbances and measurement noise; hence in this work an H^∞ parameter identification technique has been adopted wherein stability and control derivatives critically related to icing are estimated. Along with

these parameter estimates, a rich array of measurements are available that contain information on the icing degradation, including steady-state characterization, hinge moment sensing, and environmental, aerodynamic, and icing sensor information. The IMS also incorporates this information in the "sensor fusion" function referred to in.[2] Based on this information, the IMS provides (i) an initial indication of the presence of ice accretion that relies heavily on ice probe measurements, if they are available, followed by (ii) a characterization of the type and severity of the degradation of the flight dynamics, where by "type" we mean to discriminate between, for example, effects leading to tailplane stall and those leading to roll upset. Based upon this characterization, the flight envelope will be adjusted and control laws may be reconfigured.

ICING CHARACTERIZATION

In,[7] we have advocated a neural network that characterizes degradation of the aircraft flight dynamics based upon sensor data and parameter estimates. This characterization may be accomplished through a variety of other methods, but neural networks are used because of their ability to extract information simultaneously from multiple data sources that depend on the desired information in a complex manner. It is already known[8] that a feed-forward neural network with at least one hidden layer is able to approximate any continuous function to an arbitrary level of accuracy on any bounded set given ideal training. Neural networks also have inherent parallel properties that provide a robust and fault-tolerant structure. Networks are practical for aircraft applications because, following initial training, they process information very rapidly. Rapid computation can be achieved because the majority of mathematical operations involve addition, subtraction, or multiplication.

Previous work by the authors, reported in,[7] applied neural networks to icing detection and classification during a normal operational maneuver modeled as an elevator doublet. In that case, the neural networks incorporated only longitudinal stability and control derivative estimates, as the estimates were fairly accurate even in the presence of disturbances and measurement noise due to the excitation of the maneuver. In this limited scenario, neural networks were found to provide an accurate icing indication along with a less accurate but still sufficient classification of the icing severity.

In this study, we address the more common steady-level flight conditions, where the absence of excitation due to pilot input limits the effectiveness of parameter identification. Even so, it has been shown that excitation due to turbulence can be exploited to provide useful parameter estimates, albeit estimates that converge much more slowly.[6] In general, a longer delay in icing indication is more acceptable during steady level flight than during a maneuver since precipitation of an icing event is less likely in the absence of pilot action. Moreover, in this paper we address the sensor fusion function of the IMS by incorporating, in simulation, information not taken advantage of in the previous work.[7] Whereas environmental and ice probe measurements primarily provide information on the *rate* of ice accretion, increased hinge moments and steady-state effects provide information on icing degradation.[9] By steady-state effects, we mean specifically changes in trim conditions consistent with increased drag and decreased lift characteristic of icing events during flight conditions with minimal aircraft accelerations (*e.g.*, steady, level flight). The unpredictability of ice shedding and the highly complex nature of the dependence of flight dynamics degradation on the shape, roughness, and location of ice makes correlation of the ice accretion rate and the flight dynamics degradation due to icing difficult. While future efforts will be made to incorporate traditional atmospheric and ice probe measurements, we are focusing now on demonstrating the feasibility of the more novel aspects of the IMS approach. Hence in this paper we incorporate only the steady-state characterization and hinge moment sensing along with the parameter estimates into the icing characterization. Finally, we again restrict our attention to longitudinal dynamics.

Neural Network Approach

As with the previous neural network results, we take the icing severity factor η as a measure of the degradation of the flight dynamics due to ice accretion. However, for the sake of clarity, we normalize η by the nominal icing condition that corresponds to the NASA Tailplane Icing Program simulated icing condition.[10*] Since η is actually a measure of the cumulative potential atmospheric icing severity for an aircraft, the use of η as a measure of the flight dynamics degradation is consistent with the assumption that no ice shedding (due to activation of the ice protection system, for example) occurs. Furthermore, we are largely ignoring the complex relationship between atmospheric conditions on the one hand and flight dynamics degradation on the other. At present, the icing severity factor is the best measure of icing degradation available, and hence we adopt it despite its limitations in this capacity. As in,[9] we address icing encounters during periods of steady, level flight wherein the icing severity increases linearly over ten minutes from an initial clean condition.

A block diagram of the IMS is depicted in Figure 2. In the upper left corner of the figure, the flight dynamics are subject to the unknown turbulence and measurement noise input. As discussed in[5,6] these unknown exogenous signals fundamentally limit the

*In[9] this nominal icing condition corresponds to a value of $\eta = 0.0675$.

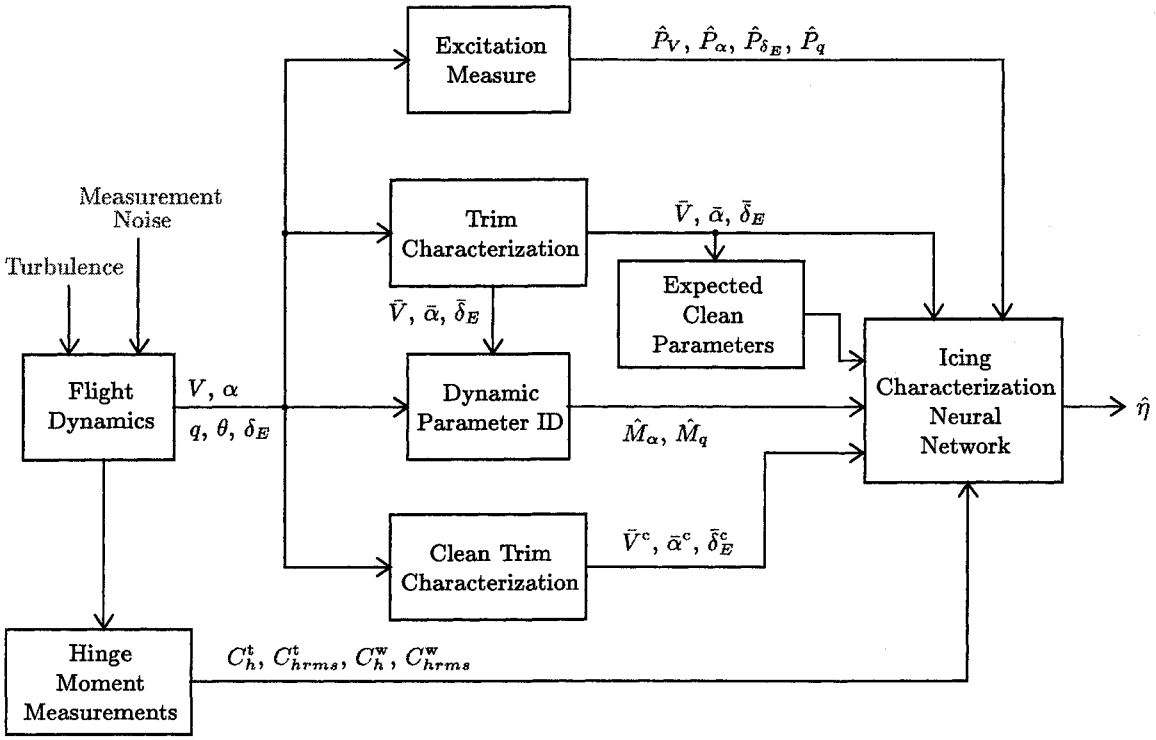

Fig. 2 IMS neural network block diagram.

accuracy of the parameter estimates, and hence must be included in any realistic simulation. From the flight dynamics we have measurements of the wing and tail hinge moments C_h^w and C_h^t along with corresponding root-mean-square hinge moment measurements C_{hrms}^w and C_{hrms}^t. The hinge moment model is described in.[11] From the flight dynamics, we also have measurements of total velocity V, angle of attack α, pitch rate q, pitch angle θ, and elevator angle δ_E. From these measurements we estimate the flight dynamics trim velocity $\bar{V}$, trim angle of attack $\bar{\alpha}$, and trim elevator angle $\bar{\delta}_E$ by lowpass filtering the corresponding measured signals at 1/30 Hz. This estimated trim is used by the dynamic parameter identification as well as being provided to the neural network directly, since the H^∞ ID algorithm is based on a dimensional derivative flight dynamics model[5] and hence depends upon the flight dynamics trim condition. The trim conditions are also used to calculate the expected clean S/C derivatives M_α^c and M_q^c against which the estimated S/C derivatives $\hat{M}_\alpha$ and $\hat{M}_q$ must be compared in order to ascertain icing degradation. Furthermore, expected clean-aircraft trim values $\bar{V}^c$, $\bar{\alpha}^c$, and $\bar{\delta}_E^c$ must be calculated to provide a reference for interpreting the estimated trim values. In the following simulations, the initial trim values are used as expected clean trim, consistent with steady, level flight scenarios. When more general scenarios are considered in the future, a more sophisticated calculation of expected clean trim will have to be included. Since the dynamic identification algorithm is expected to perform better under larger excitation and the steady-state characterization is expected to have better accuracy under smaller excitation, we have also calculated measures of excitation in order to aid the neural network in discriminating between dynamic parameter ID and steady-state characterization. As excitation measures we use an estimate of the dynamic portion of the power of the measured signals, denoted as $\hat{P}_\alpha$, $\hat{P}_V$, $\hat{P}_q$, and $\hat{P}_{\delta_E}$ and calculated according to

$$\begin{aligned}
\hat{P}_\alpha &= (\alpha - \bar{\alpha})^2, \\
\hat{P}_V &= (V - \bar{V})^2, \\
\hat{P}_{\delta_E} &= (\delta_E - \bar{\delta}_E)^2, \text{ and} \\
\hat{P}_q &= q^2.
\end{aligned}$$

The excitation measures and all other input to the neural network are lowpass filtered by batch averaging each signal over the past 1/2 second in order to reduce the effect of measurement noise. Finally, the neural network provides an estimate of the icing severity $\hat{\eta}$ at any given time instant t based only on the lowpass filtered input at that time t. In summary, the neural network incorporates the following batch filtered input

- *hinge moment measurements*: wing and tail hinge moments C_h^w and C_h^t and rms wing and tail hinge moments C_{hrms}^w and C_{hrms}^t;
- *steady-state characterization*: estimated trim values $\bar{V}$, $\bar{\alpha}$, and $\bar{\delta}_E$ and expected clean trim values $\bar{V}^c$, $\bar{\alpha}^c$, and $\bar{\delta}_E^c$

- *dynamic parameter identification*: estimated S/C derivatives M_α and M_q and expected clean S/C derivatives M_α^c and M_q^c
- *excitation measure*: $\hat{P}_\alpha$, $\hat{P}_V$, $\hat{P}_q$, and $\hat{P}_{\delta_E}$

In order to be useful, the neural network must provide accurate icing characterizations over a broad range of trim conditions and turbulence intensity. Furthermore, the icing characterization network must accurately identify clean aircraft in order to avoid false alarms. The neural networks are applied in 600-s simulations modeling a rich set of steady, level flight scenarios that correspond to combinations of the following variations

- final icing severity levels of 0, 0.02, 0.04, 0.06, 0.08, or 0.1,
- initial total velocities of 60, 65, 70, or 80 m/s,
- tail-only icing or wing and tail icing,
- turbulence level standard deviations of 0, 0.15, or 0.3 g, and
- two each of turbulence and measurement noise sample paths for all cases.

Each simulation was run under the assumption of constant engine power, with a zero flight path angle (*i.e.*, level flight), and at an altitude of 2,300 m. Simulations were performed with the aid of the FDC Matlab/Simulink toolbox as described in.[9] Furthermore, measurement noise consistent with Twin Otter instrument accuracy specifications, listed in Table 1, were incorporated as zero-mean, bandlimited white Gaussian noise. The simulations provided all measurement information at a 30 Hz sample rate.

Table 1 Measurement noise intensities taken from NASA Twin Otter instrument resolution specifications as reported by Ratvasky and Ranaudo.[12]

σ_q	σ_θ	σ_α	σ_u
0.0167°/s	0.0293°	0.003°	0.076 knot

Neural Network Architectures and Analysis

As in,[7] we use a sigmoidal back-propagation neural network structure. Once the structure of a neural network is determined, the biases and weights of the nodes and connections, respectively, are determined via numerical optimization with respect to the least squares error between the known output and the network output from a suite of training data. Of the data available from the simulation cases described above, training data was obtained by sampling the measurements at 41 s intervals from each of the cases. The networks were trained using supervised learning with a back-propagation algorithm. Back propagation consists of a gradient-based approach that runs training sets through the neural network and adjusts various weights and biases until the most accurate output is given for all training sets.

Several networks were trained and tested in order to investigate the performance of the proposed IMS as well as the utility of the various sets of measurement information. The first neural network is the *IMS neural network* that was trained and tested using the hinge moment measurements, steady-state characterization, parameter identification, and excitation. A second *limited IMS neural network* was trained and tested on all but the hinge moment measurements in consideration of (i) the possibility that hinge moment measurements are not available, and (ii) the immaturity of the hinge moment model. Next, several of neural networks were each trained and tested on individual sets of information. The accuracy of these neural networks is not considered as a prediction of the performance of the IMS, rather their performance is used to evaluate the usefulness of each information source. In this analytical capacity, we have used (i) a hinge moment neural network, (ii) a steady-state characterization neural network, and (iii) a parameter identification neural network.

For each neural network listed above, the network structure was determined via trial and error with at least three attempts at training for each. In each case the most accurate network was selected for inclusion in this paper. The architectures of each are

- *IMS network*: three hidden layers of seven nodes, twelve nodes, and five nodes, respectively,
- *Limited IMS network*: three hidden layers of nine nodes, seven nodes, and seven nodes, respectively,
- *Hinge moment network*: three hidden layers of five nodes each,
- *Steady-state characterization network*: three hidden layers of nine nodes, seven nodes, and seven nodes, respectively,
- *Parameter ID network*: three hidden layers of four nodes, five nodes, and four nodes, respectively.

NETWORK SIMULATION RESULTS

Once the networks were trained with the reduced data set, they were applied successively to each of the 150 simulation cases.† As an example, the IMS network estimates $\hat{\eta}$ as well as the actual values η are plotted for a particular simulation case of the IMS neural network in Figure 3. The general accuracy of the neural networks over the entire suite of simulation cases is measured by the root-mean-square η estimate

†Several simulation cases failed to trim successfully, and hence were discarded.

error and can be graphically depicted by a scatter plot such as in Figure 4 where the η estimate at each sample instant is plotted versus the actual η value at that instant for the IMS network. Furthermore, we have estimated the error distribution of each network over all simulation sample instants (*i.e.*, 0-600s at 30 Hz) by calculating a histogram. Figure 5 displays a histogram for the IMS neural network.

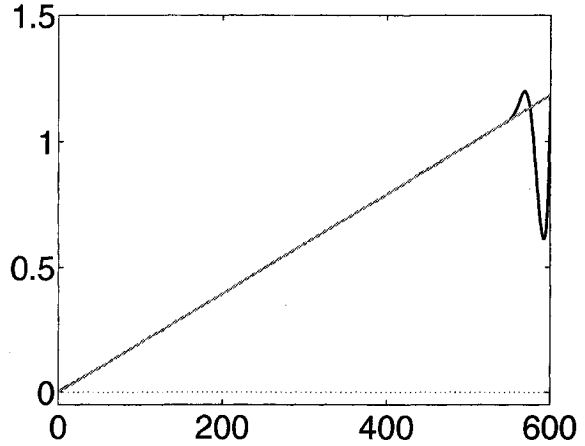

Fig. 3 *IMS neural network* η estimate along with actual value of η for a sample simulation. This simulation had an initial velocity of 70 m/s, an initial altitude of 2,300 m, both wing and tailplane icing, and no turbulence.

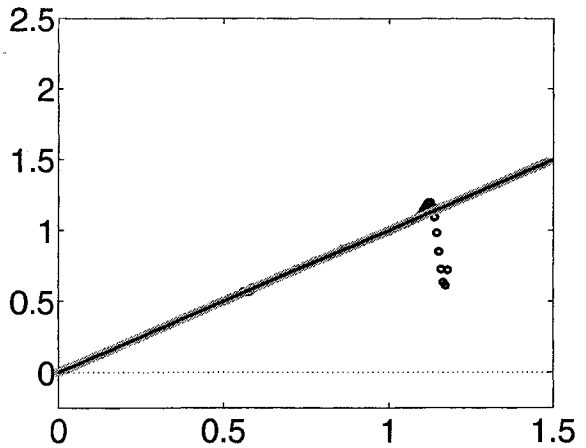

Fig. 4 Scatter plots of *IMS neural network* estimated η versus actual (instantaneous) η over all simulation runs. A perfect neural network would have all points lying on the depicted line of slope one.

Although the icing severity estimate for the IMS neural network can have significant error at a given sample instant as shown in Figure 3, Figures 4 and 5 clearly indicate that these significant errors are rare in the set of all simulation sample instants. In fact, detailed study of all simulation cases for the IMS network, which are not included here for the sake of brevity, reveal that the simulation case depicted in Figure 3 is the worst case in terms of estimate error, and moreover that all other cases appear perfect on visual inspection. The IMS network has a mean error of -2.8×10^{-6}, an error standard deviation of 4.4×10^{-4}, and an error of greater than 0.01 (*i.e.*, 1% of the difference between a clean aircraft and a nominally iced aircraft) for only 0.05% of simulation time instants. This exceptional performance, along with the immature nature of the hinge moment model, begs the question: which measurements are responsible for the performance?

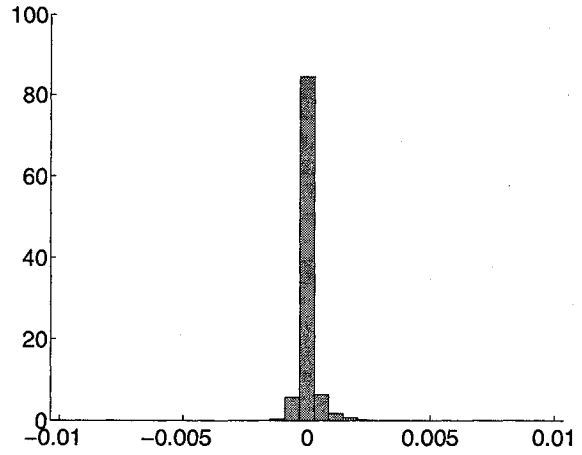

Fig. 5 Distribution of the η estimate error for the *IMS neural network* over all simulation runs expressed in terms of percentage. The distribution has mean of -2.8×10^{-6} and standard deviation of 4.4×10^{-4}.

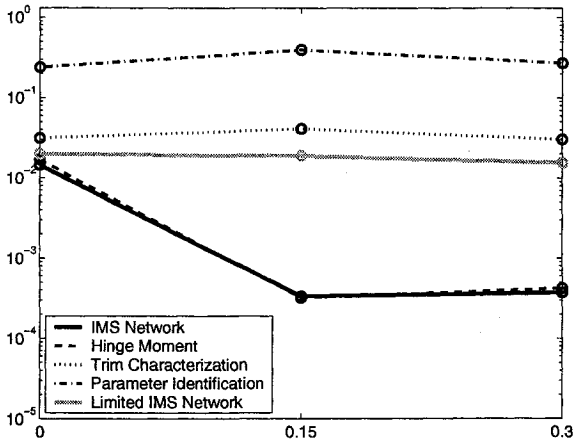

Fig. 6 Root-mean-square η estimate error versus turbulence level (in g) for several neural networks trained on various information sources. The IMS network is trained on all available information, and the limited IMS network uses all but the hinge moment measurements.

The answer to this question lies in Figure 6, where the root-mean-square errors for the IMS network, the limited IMS network, and three networks trained on only hinge moment measurements, only steady-state characterization, and only parameter ID are plotted as a function of the turbulence level. These results

clearly demonstrate that the hinge moment measurements are primarily responsible for the excellent accuracy of the IMS network. Furthermore, while the trim characterization performs fairly well, the parameter identification performs quite poorly. This is surprising given the results for time-varying H^∞ parameter identification for icing characterization during steady, level flight reported in.[6] This unexpected poor performance is most likely due to the trim condition variations that were not considered in the previous work, which assumed a linear model. Since the identification is based on a dimensional derivative model, the expected clean parameters can exhibit changes due to trim velocity variations that are much larger than changes in parameters due to icing. Presently the parameter identification is being converted to an algorithm based on dimensionless derivatives, thus removing to a large degree the dependence of the clean parameters upon the trim condition.

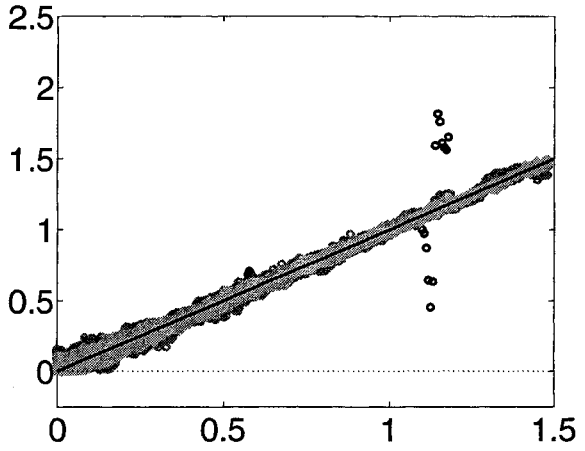

Fig. 7 Scatter plot of *limited IMS neural network* estimated η versus actual (instantaneous) η over all simulation runs. A perfect neural network would have all points lying on the depicted line of slope one.

Since the exceptional performance of the IMS network is primarily due to the hinge moment measurements, investigation of an IMS that does not rely on those measurements, *i.e.*,the limited IMS, is a natural step. A scatter plot for the limited IMS is given in Figure 7, and a distribution histogram is given in Figure 8. Although the errors for this network are clearly larger than those for the IMS network that incorporates hinge moment measurements, they are generally acceptable. As with the IMS network, the limited IMS network exhibits relatively rare large errors only very rarely. In this case, the network has a mean error of -1.8×10^{-7}, an error standard deviation of 1.7×10^{-3}, and errors larger than 10% of the difference between a clean aircraft and a nominally iced aircraft occur in only 0.37% of the sample instants. In order to provide perspective for these results, Figures 9–14 display the estimated and actual η values for several of the more inaccurate simulation cases for the limited IMS network.

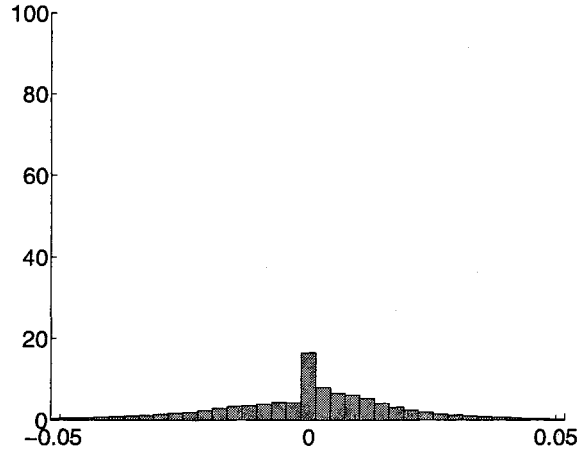

Fig. 8 Distribution of the *limited IMS network* η estimate error over all simulation runs expressed in terms of percentage. The distribution has mean of -1.8×10^{-7} and standard deviation of 1.7×10^{-3}.

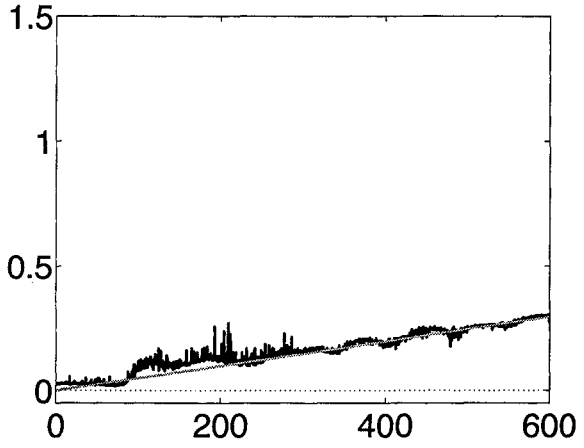

Fig. 9 *Limited IMS neural network* η estimate along with actual value of η for a simulation with an initial velocity of 70 m/s, an initial altitude of 2,300 m, both wing and tailplane icing, and a turbulence amplitude of $\sigma = 0.3g$.

CONCLUSION

This paper advocates a neural network approach for characterizing longitudinal flight dynamics degradation due to icing during steady, level flight. Consistent with previous work,[7] we have again adopted the icing severity factor η as a measure of degradation of the flight dynamics due to icing. The network incorporates (i) stability and control derivative estimates from a dynamic parameter identification algorithm, (ii) steady-state characterization based on trim condition estimates, (iii) hinge moment measurements, and (iv) measures of the excitation of the flight dynamics. The measures of excitation are included so that the network can reconcile parameter identification, which is more accurate during periods of rich excitation, and

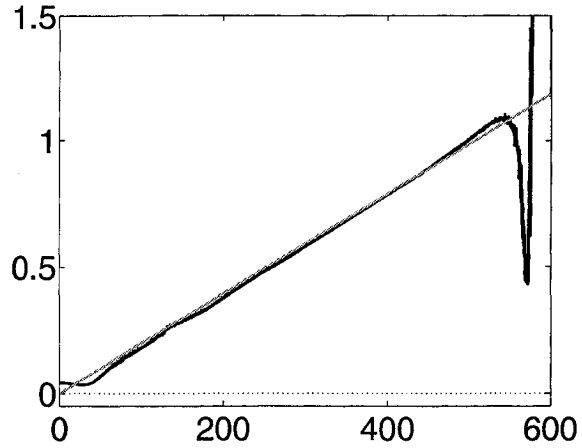

Fig. 10 *Limited IMS neural network* η **estimate along with actual value of** η **for a simulation with an initial velocity of 70 m/s, an initial altitude of 2,300 m, both wing and tailplane icing, and no turbulence.**

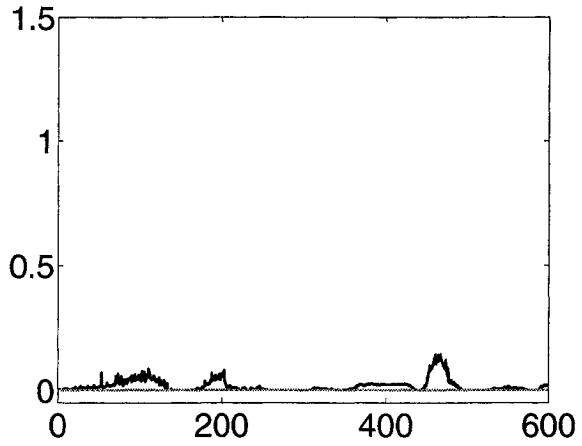

Fig. 11 *Limited IMS neural network* η **estimate along with actual value of** η **for a simulation with an initial velocity of 70 m/s, an initial altitude of 2,300 m, both wing and tailplane icing, and a turbulence amplitude of** $\sigma = 0.15g$**.**

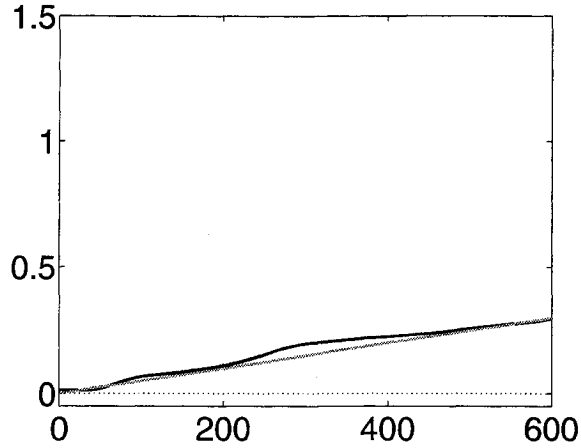

Fig. 12 *Limited IMS neural network* η **estimate along with actual value of** η **for a simulation with an initial velocity of 65 m/s, an initial altitude of 2,300 m, both wing and tailplane icing, and no turbulence.**

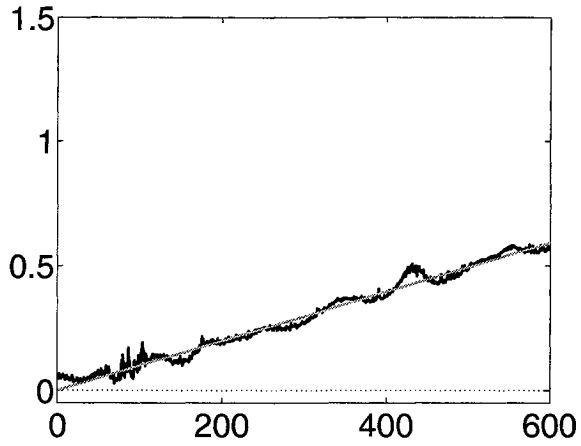

Fig. 13 *Limited IMS neural network* η **estimate along with actual value of** η **for a simulation with an initial velocity of 80 m/s, an initial altitude of 2,300 m, both wing and tailplane icing, and a turbulence amplitude of** $\sigma = 0.15g$**.**

steady-state characterization, which is more accurate during periods with less excitation. The IMS neural network was tested on a set of simulation cases that varied over a wide range of steady, level flight operating conditions. Each simulation case consisted of ten minutes of data generated at 30 Hz. The IMS network was applied to the simulated data at each time instant, and the estimated η is compared with the actual η in order to generate error statistics. The IMS network is exceptionally accurate, with η estimate errors greater than 0.01 for only 0.05% of simulation time instants, where $\eta = 0.01$ corresponds to 1% of the difference between a clean aircraft and the icing degradation corresponding to the NASA Tailplane Icing Program simulated ice.

In order to determine which class of data was most useful, we used the RMS error of networks trained on each individual data class, hinge moment measurements, steady-state characterization, and parameter identification, as a measure of the utility of that data. From this analysis, it was found that the hinge moment measurements were primarily responsible for the excellent performance of the IMS network. Moreover, the analysis demonstrated surprisingly poor parameter identification performance, despite the promising results reported previously by the authors.[6] This poor performance is most likely due to the fact that the parameter identification algorithm is based on a dimensional derivative model, and that the previous results used a linear flight dynamics model to generate simulation data. Presently, an identification algorithm based on dimensionless derivatives is being developed to address this inconsistency.

Finally, cautiousness regarding the immaturity of

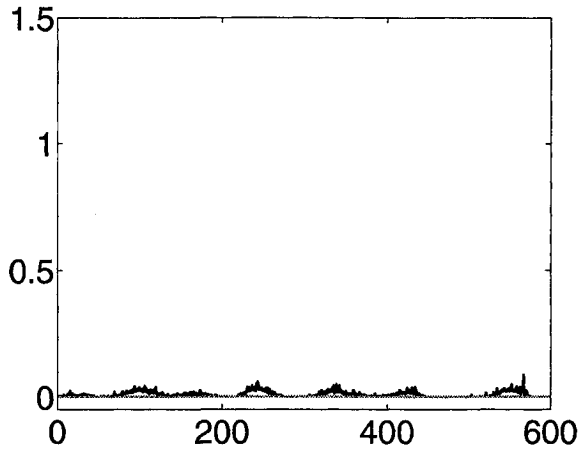

Fig. 14 ***Limited IMS neural network*** η **estimate along with actual value of** η **for a simulation with an initial velocity of 80 m/s, an initial altitude of 2,300 m, both wing and tailplane icing, and a turbulence amplitude of** $\sigma = 0.15g$.

the hinge moment model motived us to investigate a neural network that does not use hinge moment measurements. Simulation results for this *limited IMS network*, while less accurate than the IMS network, still achieve a high degree of accuracy, with η estimate errors larger than 10% of the difference between a clean aircraft and a nominally iced aircraft occurring in only 0.37% of the simulation sample instants.

ACKNOWLEDGMENT

This work was supported in part by NASA, and in part by the University of Illinois at Urbana-Champaign under the Critical Research Initiative Program. We thank Evgeniy Sklyanskiy for his effort in training dozens of neural networks and performing hundreds of network simulations.

References

[1]J. Cole and W. Sands, "Statistical study of aircraft icing accidents," in *Proc. 29th AIAA Aerospace Sciences Meeting and Exhibit*, no. AIAA–91–0558, (Reno, NV), Jan. 1991.

[2]M. B. Bragg, W. R. Perkins, N. B. Sarter, T. Başar, P. G. Voulgaris, H. M. Gurbacki, J. W. Melody, and S. A. McCray, "An interdisciplinary approach to inflight aircraft icing safety," in *Proc. 36th AIAA Aerospace Sciences Meeting and Exhibit*, no. AIAA–98–0095, (Reno, NV), Jan. 1998.

[3]"Weather investment recommendations," NASA Aeronautics Safety Investment Strategy, technical report, Apr. 1997.

[4]"Aircraft accident report, in-flight icing encounter and loss of control, ATR model 72–212, Roselawn, Indiana, October 31, 1994," National Transportation Safety Board, Technical Report NTSB/AAR-96/01, 1996.

[5]J. W. Melody, T. Başar, W. R. Perkins, and P. G. Voulgaris, "Parameter identification for inflight detection of aircraft icing," *Control Engineering Practice*, vol. 8, pp. 985–1001, Sept. 2000.

[6]J. W. Melody, T. Hillbrand, T. Başar, and W. R. Perkins, "Parameter identification for inflight detection of aircraft icing: the time-varying case," in *Proc. IFAC System Identification Symposium*, (Santa Barbara, CA), June 2000.

[7]E. A. Schuchard, J. W. Melody, T. Başar, W. R. Perkins, and P. Voulgaris, "Detection and classification of aircraft icing using neural networks," in *Proc. 38th AIAA Aerospace Sciences Meeting and Exhibit*, no. AIAA–2000–0361, (Reno, NV), Jan. 2000.

[8]K. Hornik, M. Stinchcombe, and H. White, "Multilayer feedforward networks are universal approximators," *Neural Networks*, vol. 2, no. 5, pp. 359–366, 1989.

[9]M. B. Bragg, T. Hutchison, R. Oltman, D. Pokhariyal, and J. Merritt, "Effect of ice accretion on aircraft flight dynamics," in *Proc. 38th AIAA Aerospace Sciences Meeting and Exhibit*, no. AIAA–2000–0360, (Reno, NV), Jan. 2000.

[10]T. P. Ratvasky, J. F. Van Zante, and J. T. Riley, "NASA/FAA tailplane icing program overview," in *Proc. 37th AIAA Aerospace Sciences Meeting and Exhibit*, no. AIAA–99–0370, (Reno, NV), Jan. 1999.

[11]D. Pokhariyal, M. B. Bragg, T. Hutchison, and J. Merritt, "Aircraft flight dynamics with simulated ice accretion," in *Proc. 39th AIAA Aerospace Sciences Meeting*, no. AIAA–2001–0541, (Reno, NV), Jan. 2001.

[12]T. P. Ratvasky and R. J. Ranaudo, "Icing effects on aircraft stability and control determined from flight data," in *Proc. 31st AIAA Aerospace Sciences Meeting and Exhibit*, no. AIAA–93–0398, (Reno, NV), Jan. 1993.